

# Design of Current-mode Gm-C MLF Elliptic Filters for Wireless Receivers

Xi Zhu, Yichuang Sun, and James Moritz

School of EC&EE  
University of Hertfordshire  
Hatfield, Herts, AL10 9AB, UK  
[x.zhu@herts.ac.uk](mailto:x.zhu@herts.ac.uk)

**Abstract**— Two CMOS fifth-order gm-C elliptic lowpass filters based on the current-mode multiple loop feedback (MLF) leap-frog (LF) and follow-the-leader-feedback (FLF) configurations are designed. The filters are implemented using a fully-differential linear operational transconductance amplifier (OTA). PSpice simulations using a standard TSMC 0.18 $\mu$ m CMOS process with 1.8V power supply have shown that the cut-off frequency of both filters can be tuned from 28MHz to 44MHz, dynamic range is about 67dB and 62dB for the LF and FLF filters respectively, and power consumption is about 67mW at 30MHz for both filters. Less than 0.5dB passband ripple is achieved for both filters; 65dB and 50dB stopband attenuations are obtained for MLF LF and FLF configurations, respectively.

## I. INTRODUCTION

The continuous-time filter (CTF) is one of the most important building blocks in analogue domain. It plays a very important role in many applications such as modern wireless and wired communication systems. In receivers, very demanding high-performance analogue filters are typically used to block interferers and provide anti-alias filtering before the subsequent analogue to digital conversion stage. However, it is challenging to design analogue filters with low power consumption and large dynamic range [1-3].

There are three types of filter, which have been widely developed: switched-capacitor, active-RC, and gm-C filters. Switched-capacitor filters are popular owing to excellent accuracy, but the switching noise and clock feed-through degrades the performance of the filter considerably in high frequency range. The signal bandwidth of next generation wireless communications such as WiMax, 802.11 exceed 30MHz. For this frequency range, gm-C solutions are generally preferred due to the more efficient operation of wideband OTA. On the other hand, the performances of the gm-C filter not only rely on the OTA, but also rely on the methodologies of filter design. There are three different methods to implement analogue filters: cascade, LC ladder simulation, and multiple loop feedback (MLF). The cascade method is not normally used for elliptic filter design due to

high sensitivity. The LC ladder simulation method has been widely used for analogue elliptic filter design. However, the LC ladder simulation suffers from the increased power consumption due to the need for extra OTAs to convert floating capacitors to grounded ones. It has been proved that the MLF structure has lower sensitivity than the cascade and less complexity than LC ladder simulations. They achieve good performance at high frequency with reduced parasitic effects and simple design methodologies [4]. However, MLF based configurations have not been used for design of elliptic filters for wireless communications in the literature. Therefore, two fifth-order current-mode elliptic lowpass filters for next generation wireless communication receivers are proposed in this paper, based on current-mode MLF FLF and LF configurations. The cut-off frequencies of the filters can be tuned from 28MHz to 44MHz, the power consumption of both filter is 67mW at 30MHz of cut-off frequency with TSMC 0.18 $\mu$ m 1.8V of power supply. The dynamic range (DR) of LF and FLF configuration is about 67dB and 62dB, respectively with -40dB total harmonic distortion (THD). The total output noise is about 270nV/ $\sqrt{\text{Hz}}$  for both configurations.

The paper is organized in the following way: The design of the OTA is discussed in Section II. The filter synthesis and architectures are described in Section III. The simulation results and conclusions are given in Section IV and V, respectively.

## II. OTA DESIGN

In general, the bandwidth of the OTA used in the filter must be much larger than the filter cut-off frequency. For high frequency filters, highly linear sophisticated OTAs are not normally considered due to not only narrower achievable bandwidth but also much more power consumption. Therefore, only single stage OTAs with no internal nodes can be used. The source degeneration OTAs have received more attention than other types of OTA due to the trade-offs between the linearity and power consumption. The large source degeneration factor can increase the linearity of the OTA. However, it also reduces

the overall transconductance. In this paper, the CMOS OTA in Figure 1 is used for the filter design to optimize the linearity and power consumption.

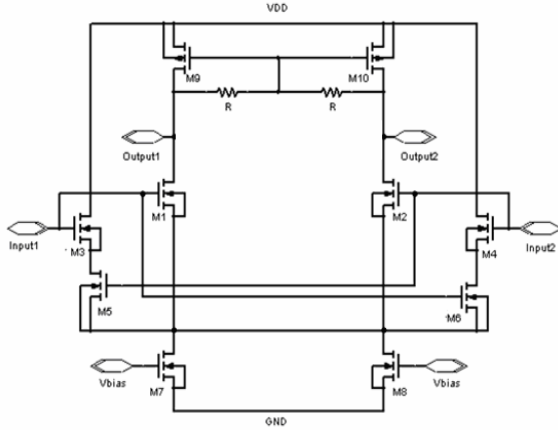


Figure 1 The basic OTA

As can be seen from Figure 1,  $M_1$  and  $M_2$  are the input transistors.  $M_3$ – $M_6$  act as active biasing circuitry in such a way that the total current drawn by  $M_3$ – $M_6$  is required for larger signals. The active biasing shares the same bias current source with the differential pair  $M_1$ ,  $M_2$ . The sizing of the transistors must be optimized for maximum linearity [5]. The two integrated resistors are used to improve the linearity of the filter, which can be replaced by triode region transistors. In order to optimize the power consumption and linearity, the aspect ratios of transistors are required to be [5]:

$$K_{1,2} : K_{3,4} = \frac{4\sqrt{X+1} + 3X - 5}{(X+1)^2} : 1 \quad (1)$$

$$K_{3,4} : K_{5,6} = X \quad (2)$$

On the other hand, the output impedance of the single stage OTA is quite low, which leads to low dc gain. The limited dc gain will result in deviations of filter performance from the desired transfer function. One example is shown in Figure 2, in which case both passband ripple and stopband attenuations are out of the specifications due to the low OTA dc gain.

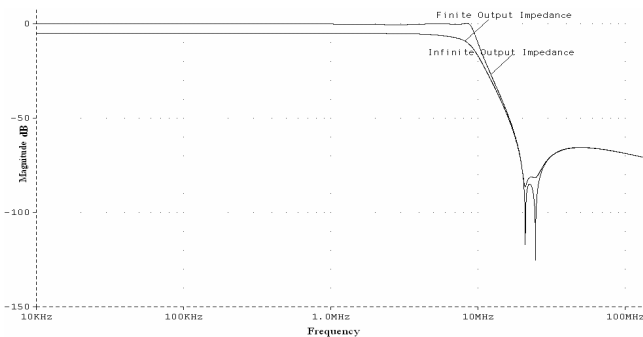


Figure 2 Comparison between the filter's ideal transfer function and the real one due to limited output impedance of OTA

Thus the output impedance of the OTA must be enhanced. This will move the low frequency pole as close as possible to dc, making it resemble an ideal integrator. One of the popular methods to increase the output impedance without introducing unwanted dominant poles is to use a negative resistance load. The idea can be illustrated using the small signal model of an OTA shown in Figure 3.

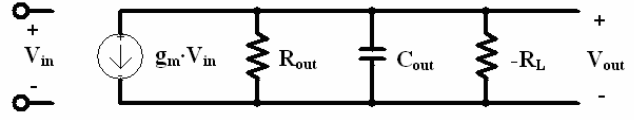


Figure 3 Small signal model of OTA with negative resistance load

The overall transfer function of Figure 3 is expressed as:

$$\frac{V_{out}}{V_{in}} = \frac{g_m}{sC_{out} + \frac{1}{R_{out}} - \frac{1}{R_L}} \quad (3)$$

From equation (3) it can be easily observed that a negative resistance load reduces the output conductance of the OTA. It can also be noticed that the negative resistance load has to be larger than the OTA output resistance to ensure that the low frequency pole lies in the left half plane. To enhance the output impedance of the OTA, a negative resistance circuit is connected to the OTA output in parallel, as shown in Figure 4.

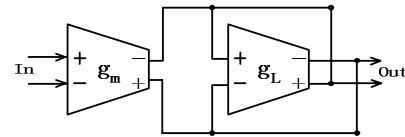


Figure 4 The diagram of simulated OTA with negative resistance

### III. FILTER ARCHITECTURE AND SYNTHESIS

We discuss current-mode MLF FLF and LF configurations based fifth-order elliptic gm-C filters, which can be used for wideband wireless communication receivers in this section. In order to generally prove the availability of current-mode MLF configurations for elliptic filter design, two different elliptic approximations are used.

#### 3.1 MLF FLF configuration

The circuit diagram of the proposed MLF FLF current-mode fifth-order elliptic lowpass filter is shown in Figure 5. The general fifth-order lowpass elliptic transfer function can be written as:

$$H(s) = \frac{A_4 s^4 + A_2 s^2 + A_0}{B_5 s^5 + B_4 s^4 + B_3 s^3 + B_2 s^2 + B_1 s + 1} \quad (4)$$

Writing the circuit current transfer function of Figure 5 and comparing this function with (4), we can establish the following equations time constants  $\tau_j = c_j/g_j$ , and zero parameters  $\alpha_j = g_{aj}/g_j$ :

$$\tau_5 = B_1, \tau_4 = \frac{B_2}{B_1}, \tau_3 = \frac{B_3}{B_2}, \tau_2 = \frac{B_4}{B_3}, \tau_1 = \frac{B_5}{B_4} \quad (5)$$

$$\alpha_1 = \frac{A_4}{B_4}, \alpha_3 = \frac{A_2}{B_2}, \alpha_5 = A_0 \quad (6)$$

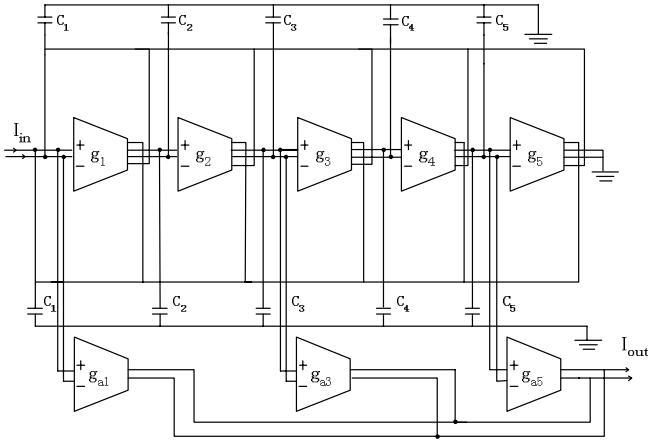


Figure 5 Fifth-order current-mode FLF elliptic filter

The normalized characteristic of a fifth-order elliptic lowpass filter is given by:

$$H_d(s) = \frac{0.0758s^4 + 0.5962s^2 + 1}{3.949s^5 + 4.58s^4 + 7.953s^3 + 5.558s^2 + 3.501s + 1} \quad (7)$$

Therefore, for the fifth-order MLF FLF elliptic lowpass filter, time constants  $\tau_j = C_j/g_j$  and zero parameters  $\alpha_j = g_{aj}/g_j$  can be calculated as using (5), (6), and (7) [6, 7]:

$$\tau_1 = 0.862, \tau_2 = 0.576, \tau_3 = 1.431, \tau_4 = 1.587, \\ \tau_5 = 3.5012, \alpha_1 = 0.02, \alpha_3 = 0.11, \alpha_5 = 1$$

The filter is designed with identical  $g_j$ 's using the CMOS OTA cell in Figure 1, with selected transconductance of 4.5mS, to improve OTA matching and facilitate design automation. The cut-off frequency of the proposed filter is chosen as 30 MHz. Using the computed  $\tau_j$  and  $\alpha_j$  values, the  $C_j$  and  $g_{aj}$  values can be calculated as:

$$C_1 = 30.12 \text{ pF}, C_2 = 19.69 \text{ pF}, C_3 = 50.85 \text{ pF}, \\ C_4 = 56.58 \text{ pF}, C_5 = 126.7 \text{ pF}, g_{a1} = 90 \text{ } \mu\text{S}, \\ g_{a3} = 495 \text{ } \mu\text{S}, g_{a5} = 4.5 \text{ mS}$$

### 3.2 MLF LF configuration

The fifth-order LF gm-C elliptic filter is shown in Figure 6. The design formulae for the LF configuration is relatively complicated compared with the FLF one. An iteration method and explicit formulas for up to sixth-order of LF filters have been derived [8]. The transfer function for the current-mode fifth-order elliptic lowpass filter in Figure 6 is given by:

$$H(s) = \frac{N(s)}{D(s)} \quad (8)$$

$$D(s) = \tau_1\tau_2\tau_3\tau_4\tau_5s^5 + \tau_2\tau_3\tau_4\tau_5s^4 \\ + (\tau_1\tau_2\tau_3 + \tau_1\tau_2\tau_5 + \tau_1\tau_4\tau_5 + \tau_3\tau_4\tau_5)s^3 \\ + (\tau_2\tau_3 + \tau_2\tau_5 + \tau_4\tau_5)s^2 + \\ (\tau_1 + \tau_3 + \tau_5)s + 1$$

$$N(s) = \alpha_1\tau_2\tau_3\tau_4\tau_5s^4 + [\alpha_1(\tau_2\tau_3 + \tau_2\tau_5 + \tau_4\tau_5) + \alpha_3\tau_4\tau_5]s^2 \\ + (\alpha_1 + \alpha_3 + \alpha_5)$$

Comparing (8) with (4), we can derive

$$\tau_1 = \frac{B_5}{B_4}, \tau_2 = \frac{B_4}{B_3 - B_2\tau_1}, \tau_3 = \frac{B_3 - B_2\tau_1}{B_2 - (B_1 - \tau_1)\tau_2} \quad (9)$$

$$\tau_4 = \frac{B_2 - (B_1 - \tau_1)\tau_2}{B_1 - \tau_1 - \tau_3}, \tau_5 = B_1 - \tau_1 - \tau_3,$$

$$\alpha_1 = A_4 / B_4, \alpha_3 = [A_2 - 2\alpha_1B_2] / \tau_4\tau_5, \quad (10) \\ \alpha_5 = A_0 - (\alpha_1 + \alpha_3)$$

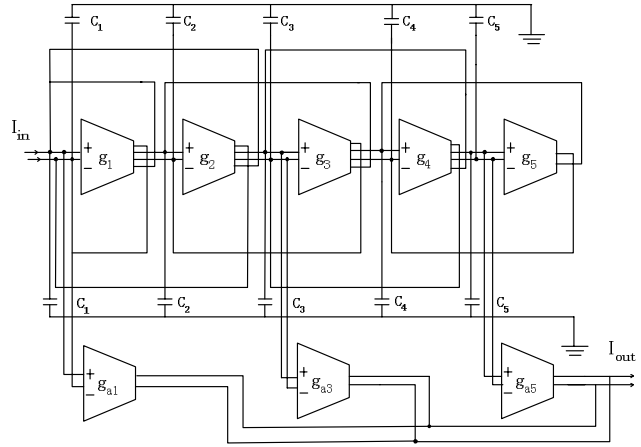


Figure 6 Fifth-order current-mode LF elliptic filter

Following the same procedure as FLF filter design, for the normalized elliptic approximation of different transition attenuation,

$$H_d(s) = \frac{0.0271s^4 + 0.324s^2 + 1}{4.692s^5 + 5.469s^4 + 9.263s^3 + 6.369s^2 + 3.839s + 1} \quad (11)$$

Using (9-11) we can calculate:

$$\tau_1 = 0.858, \tau_2 = 1.44, \tau_3 = 1.829, \tau_4 = 1.802, \tau_5 = 1.152, \\ \alpha_1 = 0.004, \alpha_3 = 0.132, \alpha_5 = 0.864$$

For the identical  $g_j$ , ( $j=1$  to 5) of 4.5mS, we can further calculate:

$$C_1 = 31.27 \text{ pF}, C_2 = 52.48 \text{ pF}, C_3 = 66.66 \text{ pF}, \\ C_4 = 65.68 \text{ pF}, C_5 = 41.99 \text{ pF}, g_{a1} = 18 \text{ } \mu\text{S}, \\ g_{a3} = 594 \text{ } \mu\text{S}, g_{a5} = 3.9 \text{ mS}$$

## IV. SIMULATION RESULTS

The two filters were designed and simulated using BSIM 3v3 Spice models for a TSMC 0.18 $\mu$ m CMOS process

available from MOSIS [9]. Figures 7 and 8 shows the magnitude responses of the FLF and LF filter, respectively. The highlighted passband ripples are given in Figures 9 and 10. As can be seen from Figures 9 and 10, the pass band ripples are about 0.5dB for both filters, and the stopband attenuations of the FLF and LF filters are about 50dB and 65dB, respectively, which matches the expected goals. The cut-off frequencies of both filter configurations can be tuned from 28MHz to 44MHz. The total power consumption of both filters is about 67mW at 30MHz cut-off frequency for a single 1.8V power supply.

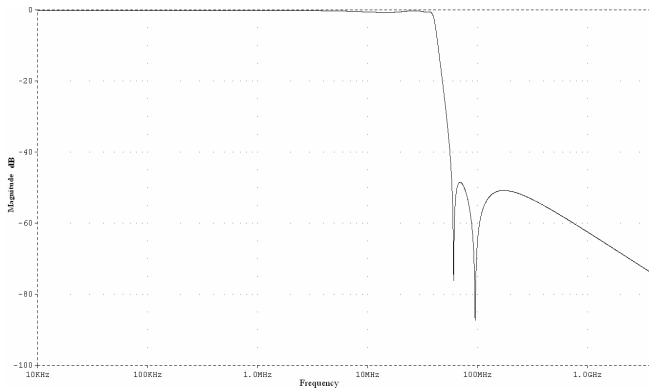


Figure 7 Magnitude response of current-mode fifth-order FLF elliptic filter

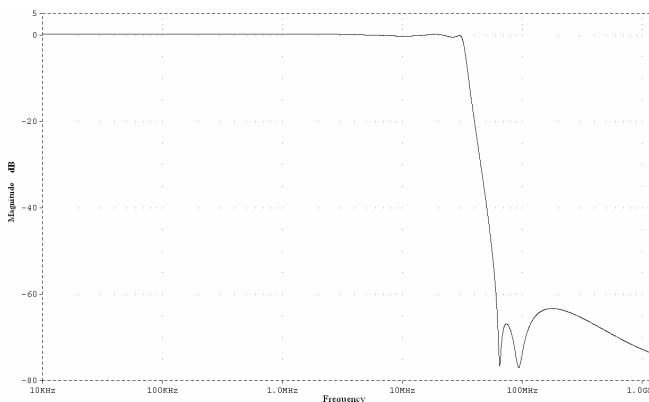


Figure 8 Magnitude response of current-mode fifth-order LF elliptic filter

Simulations of the filters have also shown a THD of less than 1% with a single tone of 600 $\mu$ A at 10MHz. The DR of LF and FLF configurations is about 67dB and 62dB, respectively with 1% of THD. Total output noise is about 270nV/ $\sqrt$ Hz for both configurations.

## V. CONCLUSIONS

Two CMOS current-mode fifth-order elliptic lowpass filters based on MLF FLF and LF configurations have been described in this paper. A linear OTA with a typically large transconductance has been used. PSpice simulations using a standard TSMC 0.18 $\mu$ m CMOS process with 1.8V power supply have shown that the cut-off frequency of both filters can be tuned from 28MHz to 44MHz, dynamic range is about 67dB and 62dB for the LF and FLF filters

respectively, and power consumption is about 67mW at 30MHz for both filters. Less than 0.5dB passband ripple is achieved for both filters; 65dB and 50dB stopband attenuations are obtained for MLF LF and FLF configurations, respectively. Therefore, it has demonstrated that the current-mode MLF LF and FLF configurations are suitable for elliptic filter design and the proposed filter can be used for advanced wireless receivers.

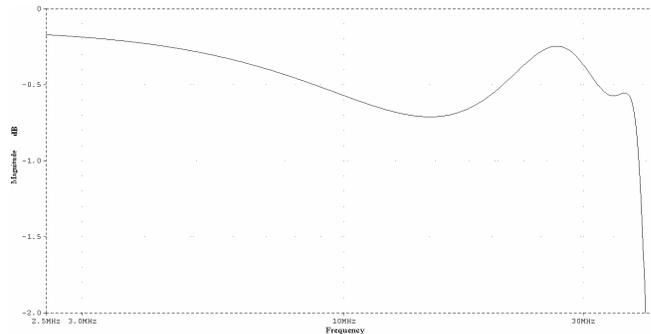


Figure 9 The passband ripples of Figure 7

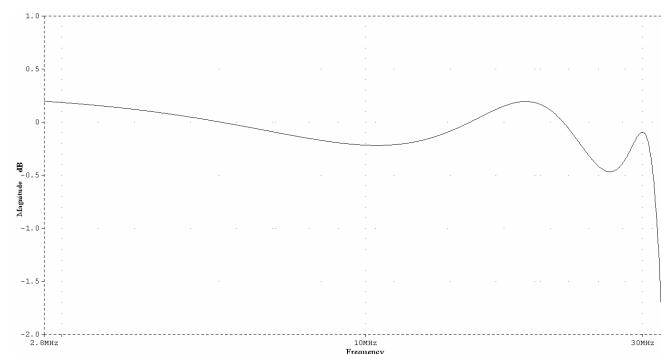


Figure 10 The passband ripples of Figure 8

## REFERENCES

- [1] Y. Sun, Edited : Wireless Communication Circuits and Systems, IEE, London, UK, 2004.
- [2] A. J. Lewinski, and J. Silva-Martinez, "A 30MHz fifth-order elliptic low-pass CMOS filter with 65-dB spurious-free dynamic range," IEEE Trans. Circ. Syst. I: regular papers, Vol. 54, No. 3, March 2007.
- [3] J. Glinianowicz, S. Szczepanski and Y. Sun, "High-frequency two-input CMOS OTA for continuous-time filter applications," IEE Proc. Circuits Devices Syst., Vol. 147, No. 1, pp. 13-18, Feb. 2000.
- [4] T. Deliyannis, Y. Sun, and J. K. Fidler: Continuous-time Active Filter Design, CRC press, Florida, USA, 1999.
- [5] C. S. Kim, Y. H. Kim, and S. B. Park, "New CMOS Linear Transconductor," Electron. Lett., Vol. 28, no. 21, pp. 1962-1964, Oct. 1992.
- [6] Y. Sun and J. K. Fidler, "General current-mode MLF MO-OTA-C filters," Proc. ECCTD, Circuit Theory and Design, Vol.2, pp. 803-805, Italy, Aug. 1999.
- [7] Y. Sun and J. K. Fidler, "Current-mode OTA-C realisation of arbitrary filter characteristics," Electronics Letters, Vol. 32, No. 13, 20<sup>th</sup> June 1996.
- [8] Y. Sun, "Synthesis of leap-frog multiple loop feedback OTA-C filters," IEEE Trans. Circ. Syst.-II, Vol. 53, No. 9, pp. 961-965, Sep. 2006.
- [9] The MOSIS Service, "Wafer Electrical Test Date and SPICE Model Parameters" <http://www.mosis.org/test/>